# Puerarin attenuates myocardial ischemia-reperfusion injury by inhibiting myocardium pyroptosis via the NRF2/HO-1 signaling pathway

XIAOYU ZHENG[1], JINPING LI[2], TIANYANG HU[3], LI TAN[1], DING LAN[1] and YING DENG[4]

[1]Department of Cardiovascular and Cerebrovascular Diseases, School of Clinical Medicine, Chongqing Medical and Pharmaceutical College, Chongqing 401331, P.R. China; [2]Department of Science and Education, The First People's Hospital of Zhaotong City and Zhaotong Hospital Affiliated to Kunming Medical University, Zhaotong, Yunnan 657000, P.R. China; [3]Department of Precision Medicine Center, The Second Affiliated Hospital of Chongqing Medical University, Chongqing 400010, P.R. China; [4]Department of Cardiology, The First Affiliated Hospital of Chongqing Medical University, Chongqing 400016, P.R. China

Received August 28, 2025; Accepted January 12, 2026

DOI: 10.3892/mmr.2026.13824

**Abstract.** Myocardial ischemia-reperfusion injury (MIRI) can trigger inflammatory responses and cause pyroptosis. Puerarin (Pue), as a traditional medicine, exhibits potential value in cardiac protection. However, the mechanism by which Pue regulates pyroptosis in MIRI remains to be fully elucidated. The present study aimed to explore the cardioprotective effects of Pue against MIRI and reveal the underlying mechanisms of these effects. Sprague-Dawley rats were used to establish *in vivo* models of MIRI, while H9C2 rat embryonic cardiomyocytes were employed as *in vitro* models. Echocardiography was performed to measure cardiac function. Triphenyltetrazolium chloride/Evans blue staining, hematoxylin-eosin staining, Masson's trichrome staining and immunohistochemistry were employed to assess the pharmacodynamic effects of Pue. The expression of molecules related to pyroptosis, such as nuclear factor E2-related factor 2 (NRF2) and heme oxygenase-1 (HO-1) were detected by immunofluorescence, Hoechst 33342/PI staining, reverse transcription-quantitative PCR and western blot analyses. The results of the present study showed that Pue pretreatment reduced the area of myocardial infarction and decreased the expression of pyroptosis-related molecules. Additionally, Pue was shown to reverse $H_2O_2$-induced mitochondrial dysfunction in cardiomyocytes and inhibit nucleotide-binding oligomerization domain-like receptor family pyrin domain-containing 3 (NLRP3)/caspase-1/gasdermin D (GSDMD)-mediated pyroptosis. Pue was also shown to stimulate the nuclear translocation of NRF2 and increase the expression of HO-1. Furthermore, Pue further demonstrated its anti-pyroptotic effects by activating the NRF2/HO-1 pathway. The present study revealed that Pue can protect injured myocardium after MIRI by inhibiting NLRP3/caspase-1/GSDMD-mediated pyroptosis. The mechanism of action for these cardioprotective effects relied upon downregulation of the NRF2/HO-1 signaling pathway. The findings of the present study provided a novel strategy for the clinical application of puerarin in the treatment of MIRI.

*Correspondence to:* Professor Ying Deng, Department of Cardiology, The First Affiliated Hospital of Chongqing Medical University, 1 Youyi Road, Yuzhong, Chongqing 400016, P.R. China
E-mail: 216129@hospital.cqmu.edu.cn

*Key words:* puerarin, pyroptosis, myocardial ischemia-reperfusion injury, nuclear factor E2-related factor 2, heme oxygenase-1, inflammation

## Introduction

Myocardial ischemia-reperfusion injury (MIRI) is a notable complication associated with interventional therapies for cardiovascular diseases, such as acute myocardial infarction. MIRI can impair both cardiac systolic and diastolic functions, leading to arrhythmias and deteriorated cardiac function (1). The pathophysiological mechanism of MIRI is complex and may involve multiple factors, including intracellular calcium overload, production of oxygen free radicals, inflammatory responses and apoptosis, all of which contribute to myocardial injury and are associated with adverse clinical outcomes (2,3). Therefore, it is important to further elucidate the underlying mechanisms of MIRI and explore new therapeutic strategies. Pyroptosis, a form of regulated cell death characterized by cellular lysis, exacerbates inflammatory cascades by releasing pro-inflammatory cytokines (4,5). During MIRI, the release of inflammatory mediators, including nucleotide-binding domain leucine-rich repeat (NLR) family proteins, caspases-1/4/5/11 and interleukin (IL)-1β, trigger pyroptosis, resulting in cell death (6). Consequently, targeting the inhibition of pyroptosis represents a promising therapeutic strategy for MIRI.

Puerarin (Pue) is a natural plant-derived medicine extracted from the root of *Pueraria lobata*, which exhibits multiple pharmacological effects, such as lactate reduction, anti-inflammatory action and pro-angiogenic activity. Pue also demonstrates therapeutic potential for cardiovascular disease,

osteoporosis, neurological diseases and intestinal fat absorption (7-9). A previous study has demonstrated that targeted delivery of the Pue herbal monomer exerts anti-pyroptotic effects by suppressing the nucleotide-binding oligomerization domain-like receptor family pyrin domain-containing 3 (NLRP3)/caspase-1/IL-1β/18 signaling pathway in a rat model of myocardial infarction, promoting macrophage polarization to the anti-inflammatory M2 phenotype and thereby alleviating the inflammatory microenvironment (10). Pue has been shown to exhibit notable suppression of pyroptosis in cardiomyocytes (11), but its role in regulating pyroptosis in MIRI requires further investigation.

The nuclear factor E2-related factor 2 (NRF2)/heme oxygenase-1 (HO-1) signaling pathway is an important intracellular antioxidant stress signaling pathway that maintains the redox balance in cells and protects them from oxidative damage (12). NRF2 binds to antioxidant response elements (AREs), for which HO-1 is a downstream target gene. Thus, the NRF2/HO-1 axis mediates cell responses to oxidative stress. Oxidative stress results in the notable generation of reactive oxygen species (ROS), triggering NLRP3 inflammasome-mediated pyroptosis and aggravating cell damage (13). Oxidative stress can be ameliorated and ROS can be suppressed by activating NRF2 (14). Furthermore, *in vitro* experiments have demonstrated that Pue activates NRF2 and reduces ROS levels in cardiomyocytes (15). Therefore, based on current findings, the present study hypothesized that NRF2 activation may have modulated pyroptosis, while Pue was hypothesized to display a dual regulatory effect on NRF2 signaling and pyroptosis. However, the mechanism by which Pue regulates pyroptosis requires exploration.

## Materials and methods

*Animal model establishment*. A total of 32 male Sprague-Dawley rats (age, 8-10 weeks; weight, 250-300 g) were purchased from Changzhou Kavens Experimental Animal Co., Ltd. All protocols in the present study strictly complied with ethical guidelines for animal research (16), and the animal experiment procedures were reviewed and approved by the Ethics Committee of Chongqing Medical University (Chongqing, China; approval no. IACUC-CQMU-2024-0618). The rats were supplied with food and water *ad libitum* and were housed in conditions maintained at a temperature range of 22-25˚C and a relative humidity of 50-60% under a 12-h light/dark cycle.

Following 1 week of acclimation, the rats were anesthetized with 50 mg/kg pentobarbital sodium intraperitoneally. An incision was made on the neck of each rat, after which the trachea was exposed by separating the muscle. A transverse incision of 1 mm was made in the cricoid cartilage and a tracheal tube was subsequently inserted and connected to a small animal ventilator for positive pressure ventilation. The ventilator parameters were adjusted in order to maintain the respiratory rate at 80 breaths/per min. The heart was exposed and the pericardium was carefully dissected. A needle was inserted 1-2 mm below the lower edge of the left atrial appendage and out of the pulmonary artery cone. The myocardium gradually became pale and ST-segment elevation was measured via electrocardiogram. After 30 min of left anterior descending artery ligation, the sutures were loosened and reperfusion was performed for 120 min. The sham operation group only underwent thoracotomies without suture ligation of arteries. A total of 100 mg/kg Pue (cat. no. P111270; Shanghai Aladdin Biochemical Technology Co., Ltd.) and 10 mg/kg pyroptosis inhibitor MCC950 (cat. no. S7809; Selleck Chemicals) were intraperitoneally injected 24, 12 and 2 h before ischemia/reperfusion (I/R), respectively. The rats were randomly divided into sham, I/R, Pue + I/R and MCC950 + I/R groups (n=8 per group). An equal volume of 0.9% saline solution was administered intraperitoneally to both the sham and I/R groups.

The health and behavior of rats were monitored every 4 h during the first 24 h after operation and twice daily thereafter. Myocardial tissues were harvested immediately after the rats were euthanized at 72 h after myocardial I/R. The human endpoints in the current study were as follows: i) Weight loss reached ≥20% and a reduction in food and water intake by ≥40% within 3 days following MIRI; ii) the occurrence of severe breathing difficulties, paralysis or continuous convulsions; iii) rats showed an inability to obtain food or water independently; or iv) extensive tissue necrosis or uncontrollable infection occurred. The rats were sacrificed by intraperitoneal injection of 250 mg/kg pentobarbital sodium. Following euthanasia, respiratory and cardiac arrest were observed, and monitoring of these parameters was sustained for an additional 5 min to verify the successful sacrifice of rats. During surgical procedures, buprenorphine (0.05 mg/kg) was subcutaneously administered twice daily to relieve pain. The total duration of the experiment was 10 days. A total of two rats were euthanized within 24 h of reperfusion due to meeting the aforementioned endpoints and were replaced with new rats.

*Echocardiography*. Small animal echocardiography was performed using the Vevo2100 imaging system (FUJIFILM VisualSonics; FUJIFILM Corporation). Anesthesia was administered by intraperitoneal injection of 50 mg/kg pentobarbital sodium. The rats were shaved, and a 30 MHz probe was placed on the left sternal border between the 4 and 5th intercostal spaces of the left sternum. The angle was adjusted to obtain the best view, which displayed the maximum anatomical detail of the cardiac structures. Two-dimensional, M-mode and color Doppler ultrasound images were collected successively, and heart rate, left ventricular end-diastolic diameter and left ventricular end-systolic diameter were recorded. The left ventricular ejection fraction (LVEF) value was calculated. The mean value for each parameter was derived from five consecutive cardiac cycles.

*Triphenyltetrazolium chloride (TTC)/Evans blue staining*. A thoracotomy was performed on the rats after they were anesthetized with 50 mg/kg pentobarbital sodium intraperitoneally. The anterior descending coronary artery was ligated quickly, and 1 ml 0.5% Evans blue dye (cat. no. E2129; Sigma-Aldrich Co. LLC) was injected through the thoracic aorta. The heart was then isolated and preserved. The slices (1 mm) were made after the heart had been collected, stained with 1% TTC (cat. no. D025-1-3; Nanjing Jiancheng Bioengineering Institute) at 37˚C for 15-20 min in the dark, fixed in 4% formalin at room temperature for 24 h and photographed

using a light microscope (cat. no. VHX-X1, Keyence Co., Ltd.). ImageJ (version 1.8.0; National Institutes of Health) was used to analyze the myocardial infarctions.

*Hematoxylin-eosin staining (H&E) staining*. Myocardial tissue samples were fixed in 4% neutral formaldehyde at room temperature for 48 h. The tissue was dehydrated with an ethanol gradient (75% for 4 h, 85% for 2 h, 90% for 1.5 h, 95% for 1 h and absolute ethanol I/II for 0.5 h), then stained with the transparent agent xylene for transparency and placed in a paraffin tank to complete the wax immersion and embedding procedure. The wax blocks were sectioned into slices of 4 $\mu$m, which were baked at 60˚C for 3 h. The sections were dewaxed after baking. Hematoxylin staining was performed at room temperature for 5 min, before sections were washed with water for 5 min to achieve bluing. The sections were stained with 1% eosin staining solution at room temperature for 5 min and subsequently washed with water for 30 sec to complete H&E staining. After dehydration, the sections were made transparent, mounted, observed and images captured using a light microscope (cat. no. IX71; Olympus Corporation).

*Masson's trichrome staining*. The cardiac tissue was fixed, embedded and sectioned, following the aforementioned H&E staining protocol. The section thickness was 5 $\mu$m. The sections were treated with hematoxylin solution (5 min), ponceau-acid fuchsin solution (3 min), 1% phosphomolybdic acid solution (5 min) and aniline blue staining solution (all room temperature; 5 min) successively. After rinse in 1% acetic acid (1 min) and running water (30 sec), sections were dehydrated and mounted. Myocardial fibers were stained red, collagen fibers were stained blue and cell nuclei were stained dark blue. Images were captured using a light microscope (cat. no. BX53; Olympus Corporation).

*Immunohistochemistry (IHC)*. Tissues were fixed with 4% paraformaldehyde at room temperature for 24 h. Paraffin sections (4 $\mu$m) were deparaffinized in xylene (cat. no. X112054; Aladdin, Inc.), rehydration through a graded ethanol and rinsed with distilled water for 5 min. The sections were placed in a beaker containing citrate buffer as the antigen retrieval solution (cat. no. P0086; Beyotime Institute of Biotechnology), heated in a microwave at 700 W (95±3˚C) for 15 min, and then cooled naturally. Antigen retrieval was performed by rinsing with PBS three times for 5 min each. Endogenous peroxidase activity was blocked by incubating samples with 3% hydrogen peroxide at room temperature for 15 min. Then, 5% goat serum (cat. no. C0265; Beyotime Institute of Biotechnology) was added at room temperature for 30 min to prevent non-specific staining. Subsequently, diluted primary antibodies against IL-1β (1:200, cat. no. ab9722; Abcam), NLRP3 (1:5,000, cat. no. MA5-32255; Thermo Fisher Scientific, Inc.) and NRF2 (1:500, cat. no. PA5-27882; Thermo Fisher Scientific, Inc.) were added at 4˚C overnight. An HRP-labeled secondary antibody (1:500, cat. no. 7071; Cell Signaling Technology) were incubated at 37˚C for 1 h. The sections were developed using a DAB chromogenic agent (cat. no. ZLI-9018; Beijing Zhongshan Jinqiao Biotechnology Co., Ltd.), counterstained with hematoxylin at room temperature for 3 min. The sections were dehydrated, cleared with xylene and mounted with neutral balsam (cat. no. ZLI-9555; Beijing Zhongshan Jinqiao Biotechnology Co., Ltd.). Finally, sections were observed under a light microscope (cat. no. XDS-1A, Shanghai Cany Precision Instrument Co., Ltd.). Quantitative analysis was performed using ImageJ (version 1.8.0; National Institutes of Health). Brown-yellow staining indicated the positive expression of inflammasome markers.

*Cell culture and model establishment*. H9C2 rat embryonic cardiomyocytes (cat. no. ACL-0143; China Center for Type Culture Collection) were cultured in high-glucose Dulbecco's modified Eagle's medium (cat. no. SH30243.01; HyClone™; Cytiva), supplemented with 10% fetal bovine serum (cat. no. A511-001; Lonsera; Shanghai Shuangru Biotechnology Co., Ltd.) and 1% penicillin-streptomycin (cat. no. BL505A; Biosharp). The cells were cultured in a 5% $CO_2$ incubator at 37˚C. The oxidative stress model was established by treating the cells with different concentrations of $H_2O_2$ (0, 100, 200, 300 and 400 $\mu$M) for different durations (0, 15, 30, 60, 90 and 120 min) in order to screen for the optimal time and concentration for the purposes of the study. These cells were randomly divided into 3 groups: i) The control group, which consisted of normal cultured cells; ii) the $H_2O_2$ group, containing cells treated with $H_2O_2$; and iii) the Pue + $H_2O_2$ group, in which cells were pre-treated with Pue at the selected concentration of 100 mM for 2 h prior to the addition of $H_2O_2$.

*Cardiomyocyte transfection*. To overexpress NRF2 in H9C2 cardiomyocytes, 2.5 $\mu$g of pcDNA3.1-NRF2 plasmid (Gencefe) was mixed with Lipofectamine® 8000 transfection reagent (cat. no. C0533; Beyotime Institute of Biotechnology) according to the manufacturer's instructions and the empty pcDNA3.1 plasmid was used as a negative control. Cardiomyocytes were transfected for 48 h. Transfection efficiency was assessed via western blotting. The cells were then randomly divided into 5 groups (n=3 wells/group): i) The negative control overexpression (OE-NC) group, as aforementioned; ii) the $H_2O_2$ + OE-NC group, in which were transfected with empty pcDNA3.1 plasmids as a negative control and then treated with $H_2O_2$; iii) the $H_2O_2$ + NRF2 overexpression (OE-NRF2) group, comprising cells transfected with the pcDNA3.1-NRF2 plasmid and treated with $H_2O_2$; iv) the $H_2O_2$ + OE-NC + Pue group, consisting of cells transfected with the empty pcDNA3.1 plasmid, pretreated with Pue for 2 h and treated with $H_2O_2$; and v) the $H_2O_2$ + OE-NRF2 + Pue group, containing cells that were transfected with the pcDNA3.1-NRF2 plasmid, pretreated with Pue for 2 h and treated with $H_2O_2$. Temperature of transfection was 37˚C. The cells were cultured for 48 h after transfection, seeded into 96-well plates and cultured at 37˚C for an additional 24 h before subsequent experimentation.

*Cell counting kit-8 (CCK-8) assay*. A CCK-8 kit (cat. no. C0037; Beyotime Institute of Biotechnology) was used to evaluate the viability of H9C2 cells. According to the manufacturer's instructions, H9C2 cells were incubated in 96-well plates. For $H_2O_2$ toxicity curve, cells were exposed 0, 100, 200, 300 and 400 $\mu$mol/l) of $H_2O_2$ for different durations (0, 15, 30, 60, 90, 120 min). For the Pue toxicity curve, cells were incubated at 37˚C with Pue (0, 20, 40, 60, 80, 100,

120 $\mu$mol/l) for 2 h. 20 $\mu$l of CCK-8 solution was added to each well, after which samples were incubated at 37˚C in a 5% $CO_2$ incubator for 3 h in the dark. The absorbance at a 450 nm wavelength was measured using an enzyme detector (cat. no. MK3; Thermo Fisher Scientific, Inc.).

*Examination by transmission electron microscopy (TEM).* H9C2 cardiomyocytes were fixed with 2.5% glutaraldehyde at 4˚C for 2 h, centrifuged and sedimented at 90 x g for 5 min at 4˚C and subsequently fixed as aforementioned. Cells were washed 3 times with 0.1 M phosphate buffer solution (pH 7.4), each time for 15 min. Then, 1% osmium tetroxide was added to suspend the cell clusters at room temperature for 2 h. After dehydrating the tissue blocks, these were embedded in a resin-embedding agent (cat. no. 90529-77-4; Structure Probe, Inc.) at 60˚C for 48 h and sliced into ultra-thin sections of 60-80 nm. The sections were sequentially stained with 2% uranium acetate (15 min) and lead citrate solutions (both 15 min) at room temperature. The ultrastructure of the cells was observed using TEM (cat. no. HT7700; Hitachi High-Technologies Corporation).

*Measurement of lactate dehydrogenase (LDH).* The supernatant of H9C2 cardiomyocytes was collected from cells in each group. The supernatant was analyzed for LDH activity according an LDH activity kit (cat. no. BC0680; Beijing Solarbio Science & Technology Co., Ltd.). The supernatant was mixed with the LDH detection working solution at a ratio of 1:1 and incubated at room temperature for 30 min in the dark. Once the reaction terminated, the absorbance was measured immediately at a wavelength of 450 nm using an enzyme detector (cat. no. MK3; Thermo Fisher Scientific, Inc.) to calculate LDH activity in the supernatant.

*Hoechst 33342/PI staining.* The Hoechst 33342/PI double fluorescence staining kit (cat. no. CA1120; Beijing Solarbio Science & Technology Co., Ltd.) was used to detect pyroptosis in H9C2 cardiomyocytes from each group. The Hoechst 33342/PI staining solution (5 $\mu$l) were added to each group, mixed well and incubated for 30 min at 4˚C in the dark. After washing the cells three times with PBS, samples were observed under a fluorescence microscope and images were captured. Hoechst 33342 resulted in blue fluorescence, marking all cells, while PI emitted red fluorescence, which marked dead cells. The results were analyzed using ImageJ software (version 1.8.0; National Institutes of Health).

*Immunofluorescence detection.* H9C2 cells were fixed with 4% paraformaldehyde at room temperature for 15 min, followed by permeabilization with 0.1% Triton X-100 for 10 min. Samples were blocked with 5% BSA (cat. no. ST023; Beyotime Institute of Biotechnology) at room temperature for 1 h, before the cells were incubated with NRF2 (1:200; cat. no. 16396-1-AP; Proteintech Group, Inc.), HO-1 (1:200; cat. no. 10701-1-AP; Proteintech Group, Inc.) primary antibodies at 4˚C overnight. Cells were subsequently incubated with the secondary fluorescent antibody (goat anti-rabbit cyanine 3-conjugated; 1:500; cat. no. SA00009-2; Proteintech Group, Inc.) at room temperature for 1 h in the dark. Following this, cells were incubated with Hoechst 33258 (1:1,000; cat. no. C1011; Beyotime Institute of Biotechnology) at room temperature for 15 min to stain the nuclei of the cells. Fluorescence microscopy (cat. no. BZ-X800E; Keyence Co., Ltd.) was used to observe and photograph the samples and fluorescence intensity was evaluated using ImageJ (version 1.8.0; National Institutes of Health). NRF2 and HO-1 showed positive signals in the form of red fluorescence, while the Hoechst 33258-stained nuclei of the cells exhibited blue fluorescence.

*Mitochondrial membrane potential assay.* The mitochondrial membrane potential of H9c2 cardiomyocytes was detected using the JC-1 Staining kit (cat. no. H9C2; Beijing Solarbio). Following the manufacturer's instructions, cells were incubated with JC-1 at concentration of 2 $\mu$M for 30 min at 37˚C in the dark, ensuring complete coverage of the cells. Then the cells were washed three times with pre-warmed (37˚C) PBS. Nuclei were stained with 1 ml Hoechst 33342 (cat. no. C1022; Beyotime Institute of Biotechnology) for 5 min at room temperature in the dark. Red (JC-1 aggregates) and green (JC-1 monomers) fluorescence images were observed under fluorescence microscope (cat. no. BZ-X800E; Keyence Co., Ltd.), and the red/green fluorescence intensity ratio was quantified using ImageJ (version 1.8.0; National Institutes of Health).

*RT-qPCR.* Using the TRIzol Extraction Kit (Thermo Fisher Scientific, Inc.), total RNA was extracted from rat myocardial tissues and reverse transcribed into cDNA using the RevertAid First Strand cDNA Synthesis Kit (cat. no. K1622; Thermo Fisher Scientific, Inc.). According to the manufacturer's instructions, qPCR was performed using the SYBR Green PCR kit (cat. no. F-415XL; Thermo Fisher Scientific, Inc.) on the 7500 Real-Time PCR System (Applied Biosystems; Thermo Fisher Scientific, Inc.) to evaluate mRNA expression of the target genes. Primer Premier 5.0 software (Sangon Biotech Co., Ltd.) was used for the design and synthesizing of all primers, which are shown in Table I.

*Western blotting.* Myocardial tissue and cardiomyocytes were lysed in RIPA lysis buffer (cat. no. P0013B; Beyotime Institute of Biotechnology) at 4˚C for 30 min; the supernatant was subsequently collected after centrifugation. As NRF2 is a nuclear transcription factor, its level in the nucleus was primarily detected in the present study. GAPDH was used as a loading control for cytoplasmic protein, while histone H3 was used as a loading control for the detection of nuclear NRF2. Nuclear proteins were extracted using the Nuclear and Cytoplasmic Protein Extraction Kit (cat. no. P0027; Beyotime Institute of Biotechnology) in strict accordance with manufacturer's instructions. Sample protein concentration was determined using a BCA protein concentration determination kit (cat. no. BL521A; Biosharp Life Sciences). A total of 30 $\mu$g protein/lane was loaded for electrophoresis. Proteins were separated by SDS-PAGE using a 5% stacking gel at 80 V for 30 min and 10% separating gel at 120 V for 60 min, and were transferred to PVDF membranes. To prevent non-specific binding, membranes were incubated with 5% BSA (cat. no. ST023; Beyotime Institute of Biotechnology) at 37˚C for 2 h. Subsequently, samples were incubated with NRF2 (1:1,000; cat. no. 16396-1-AP; Proteintech Group, Inc.), HO-1 (1:1,000; cat. no. 10701-1-AP; Proteintech Group, Inc.),

Table I. Primer sequences for reverse transcription-quantitative PCR.

| Gene | Sequence (5'-3') |
|---|---|
| GSDMD | F: CAGCATCCTTGAGTGTCT |
| | R: GAGCCTTAGTAGCCAGTAG |
| NLRP3 | F: TTGAAGAGGAGTGGATAGGT |
| | R: GGTGTAGCGTCTGTTGAG |
| ASC | F: ACAGCCAGAACAGAACATT |
| | R: GTCCTTCAGTCAGCACATT |
| IL-1β | F: GACAGAACATAAGCCAACAA |
| | R: ACACAGGACAGGTATAGA TTC |
| NRF2 | F: CCATTTACGGAGACCC |
| | R: CACTGTGCCCTTGAGC |
| GAPDH | F: ATCGGACGCCTGGTTA |
| | R: CGCTCCTGGAAGATGG |

F, forward; R, reverse; GSDMD, gasdermin D; NLRP3, nucleotide-binding oligomerization domain-like receptor family pyrin domain-containing 3; ASC, apoptosis-associated speck-like protein; NRF2, nuclear factor E2-related factor 2.

NLRP3 (1:1,000; cat. no. 68102-1-Ig; Proteintech Group, Inc.), apoptosis-associated speck-like protein (ASC; 1:1,000; cat. no. BD-PT0365; Biodragon), gasdermin D (GSDMD) (1:1,000; cat. no. BD-PT7991; Biodragon), caspase-1 (1:1,000; cat. no. BD-PC0003; Biodragon), IL-1β (1:1,000; cat. no. BD-PT5201; Biodragon), histone H3 (1:1,000; cat. no. abs145120; Absin) and glyceraldehyde-3-phosphate dehydrogenase (GAPDH; 1:1,000; cat. no. 60004-1-Ig; Proteintech Group, Inc.) primary antibodies overnight at 4˚C. After incubation with primary antibodies, PVDF membranes were washed three times with TBST (0.1% Tween-20) for 5 min each. The PVDF membranes were then placed in a secondary antibody solution of dilution 1:5,000 containing HRP-labeled goat anti-rabbit IgG (cat. no. ZB-2301; Beijing Zhongshan Jinqiao Biotechnology Co., Ltd.) and HRP-labeled goat anti-mouse IgG (cat. no. ZB-2305; Beijing Zhongshan Jinqiao Biotechnology Co., Ltd.) and incubated at 37˚C for 1 h. After adding ECL visualization reagent (cat. no. P0018S; Beyotime Institute of Biotechnology), the samples were placed in a chemiluminescence imaging system (cat. no. Tanon 5200; Tanon Science & Technology Co., Ltd.) for detection. The intensities of protein bands were semi-quantified using ImageJ software (version 1.8.0; National Institutes of Health).

*Statistical analysis*. Statistical analyses were performed using GraphPad Prism software (version 9.1; Dotmatics), and data were presented as mean ± standard deviation of at least 3 times. Unpaired Student's t-tests and one-way ANOVA with Bonferroni post-hoc test were used, while for two factors, two-way ANOVA with the Bonferroni post-hoc test was used instead. $P<0.05$ was considered to indicate a statistically significant difference.

## Results

*Pue preserves cardiac function in myocardial I/R rats*. To evaluate the protective effects of Pue preconditioning on MIRI, the present study established a rat model of MIRI (Fig. 1A). There were no significant differences in cardiac function parameters observed among the four experimental groups during pre-operative echocardiography. The I/R group showed significantly increases in left ventricular internal diastolic diameter and left ventricular internal diameter at systole along with significantly decreased LVEF values compared with the sham group post-operation. Therefore, Pue administration improved cardiac function in I/R model rats (Fig. 1B). TTC staining revealed that all three experimental groups showed higher myocardial infarction areas, represented by lighter reddish areas, than the sham group, with the most obvious infarction observed in the I/R group. Compared with the I/R group, both Pue and MCC950 treatments significantly reduced infarction area, suggesting that Pue intervention alleviated myocardial infarction (Fig. 1C and D).

Masson's trichrome staining of myocardial sections was performed in each group to evaluate myocardial fibrosis. In the I/R group, myocardial tissue was notably damaged. The arrangement of myocardial fibers was uneven, a number of fibers were broken or dissolved and these characteristics were also accompanied by fibrous connective tissue hyperplasia. Pue and MCC950 treatments markedly reduced the area of myocardial infarcts and inhibited myocardial fibrosis (Fig. 1E). These findings demonstrated that Pue alleviated myocardial ischemic injury by reducing the myocardial infarction area and inhibiting fibrosis, thereby restoring cardiac function after I/R injury.

*Pue inhibits inflammation and pyroptosis during myocardial I/R*. Following myocardial I/R, cardiomyocytes undergo various forms of cell death, leading to the expansion of the damaged area and the exacerbation of ischemic injury. Recent studies have demonstrated that pyroptosis is associated with myocardial I/R and depends on inflammatory mediators (4,17,18). As a result, the anti-pyroptotic effects of Pue can be observed by detecting the release of inflammatory factors. H&E staining showed notable inflammatory cell infiltration, nuclear displacement and cardiomyocyte necrosis in the I/R group compared with the sham group, which were markedly reduced in the Pue treatment group (Fig. 2A). IHC was used to assess inflammasome protein expression and localization in myocardial tissue. Compared with the sham group, the expression of NLRP3 and IL-1β in the I/R group were significantly increased, whereas these expression significantly decreased after treatments with Pue and MCC950. Since the NRF2/HO-1 pathway serves an important role in regulating the antioxidant responses of cell, IHC also demonstrated a significant increase in the expression of NRF2 in the Pue and MCC950 groups compared with the I/R group (Fig. 2B and C).

To further study the effect of Pue on inhibiting pyroptosis in MIRI, RT-qPCR and western blotting were performed to detect the expression of key pyroptosis-related markers in cardiomyocytes. Compared with the sham group, the expression levels of pyroptosis-related markers such as ASC, IL-1β, NLRP3 and GSDMD were significantly elevated in the I/R group. These

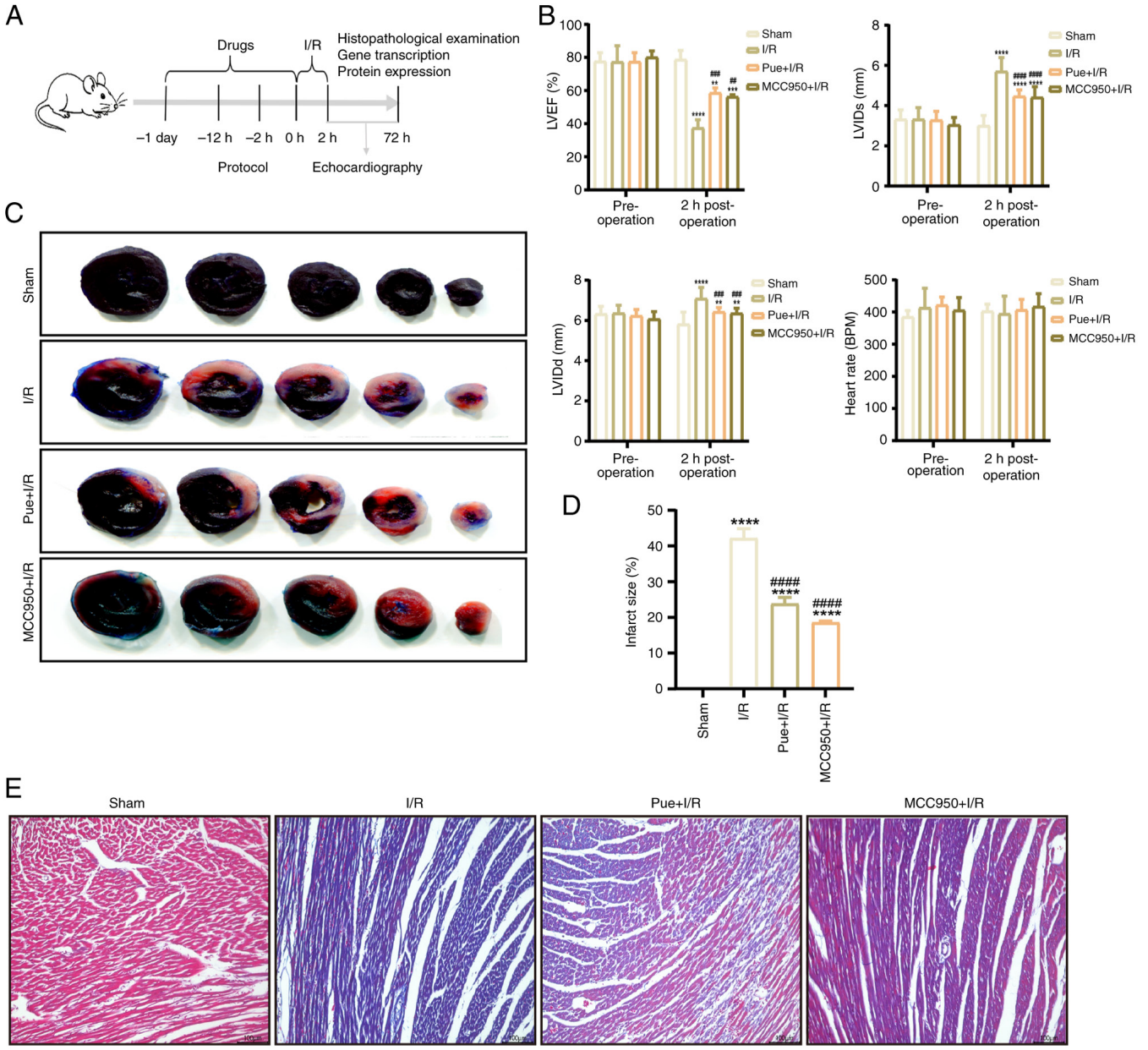


Figure 1. Pue displays cardioprotective effects against myocardial ischemia-reperfusion injury *in vivo*. (A) Timeline of Pue administration and schematic of the rat I/R injury model. (B) Changes in cardiac function (LVIDd, LVIDs, LVEF) and heart rate were observed in each group at 2 h after myocardial I/R. (C) Triphenyltetrazolium chloride staining of myocardial tissues. (D) Quantitative comparison of infarction areas among each group (n=8). (E) Masson's trichrome staining of myocardial tissues (scale bar, 100 $\mu$m). $^{**}$P<0.01, $^{***}$P<0.001 and $^{****}$P<0.0001 vs. sham group; $^{\#\#}$P<0.01, $^{\#\#\#}$P<0.001 and $^{\#\#\#\#}$P<0.0001 vs. I/R group. Pue, puerarin; LVIDd, left ventricular internal dimension at end-diastole; LVIDs, left ventricular internal dimension at end-systole; LVEF, left ventricular ejection fraction; I/R, ischemia/reperfusion.

expression levels were significantly attenuated after treatment with Pue and MCC950 (Fig. 2E). Western blot analysis showed that, compared with the sham group, the expression levels of NLRP3, ASC, GSDMD, IL-1β and caspase-1 significantly increased in the I/R group, while the expression of NRF2 and HO-1 proteins were significantly reduced in the I/R group. In the Pue + I/R group, the expression of key pyroptotic proteins was significantly decreased compared with the I/R group, whereas the expression levels of NRF2 and HO-1 were significantly increased (Fig. 2D, F-H). Based on these findings, it was possible to conclude that Pue inhibited pyroptosis and reduced MIRI, and that its mechanism may have involved the NRF2/HO-1 signaling pathway. Thus, Pue showed the potential to alleviate MIRI by regulating pyroptosis.

*Pue alleviates $H_2O_2$-induced cardiomyocyte pyroptosis*. To investigate the protective effect of Pue on cardiomyocytes under oxidative stress, H9C2 cells were exposed to $H_2O_2$ to establish an *in vitro* model of oxidative stress. Cell viability decreased in a time- and dose-dependent manner following $H_2O_2$ treatment. To ensure that the inhibition rate was within the range of 20 to 30%, $H_2O_2$ (100 $\mu$M; 120 min) was selected for subsequent experiments by CCK-8 assays (Fig. S1A and B). The present study evaluated the impact of Pue on the viability of H9C2 cells before further experiments. Pretreatment with different concentrations (20-120 $\mu$mol/l) of Pue for 2 h significantly improved cell viability in a dose-dependent manner. Finally, 100 $\mu$M Pue was selected for the following experiments

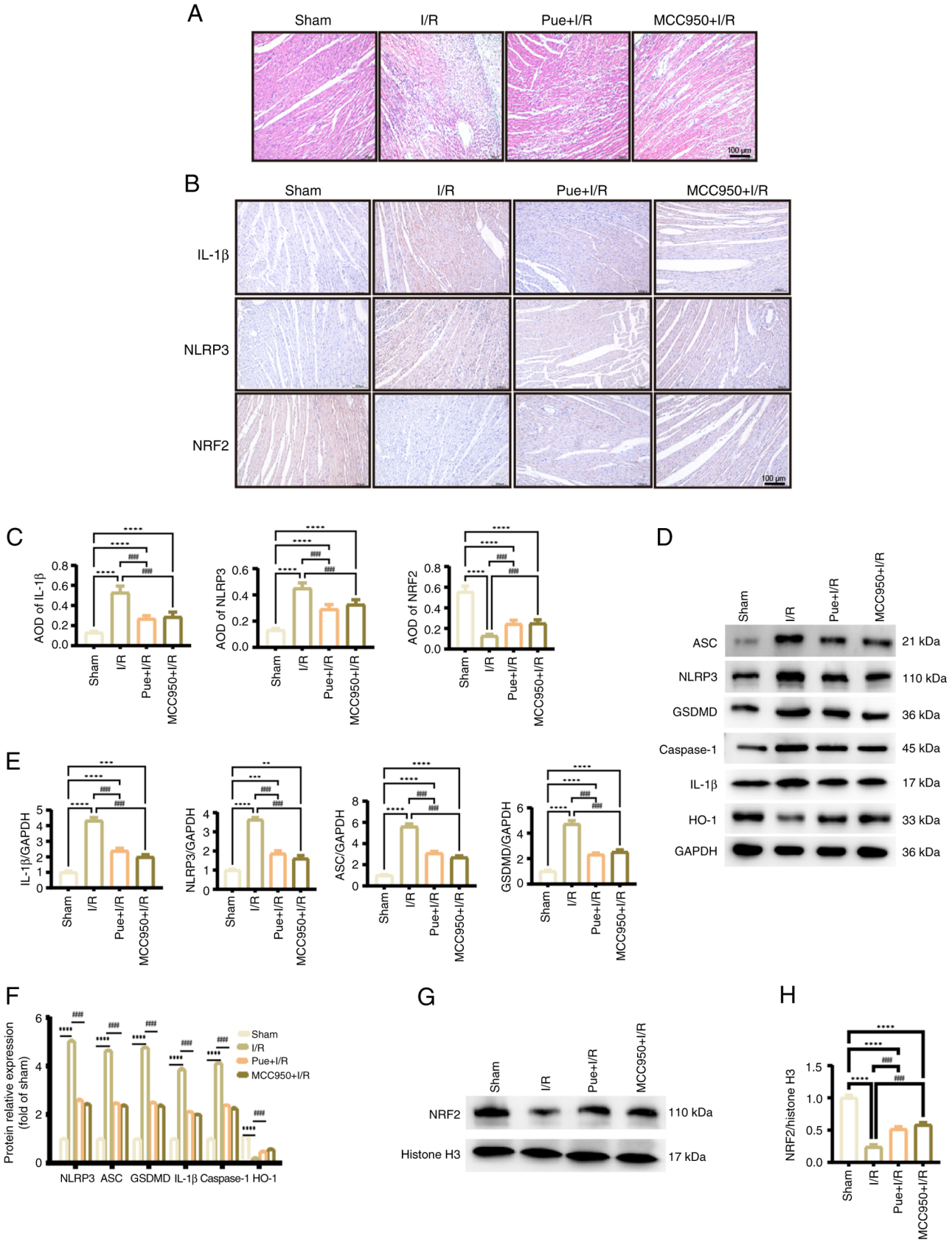


Figure 2. Pue inhibits the key proteins of the inflammasome and pyroptosis in myocardial ischemia-reperfusion injury. (A) Hematoxylin-eosin staining showed the inflammatory condition of myocardial tissue (n=8; scale bar, 100 $\mu$m). (B) Immunohistochemistry detected the positive expression of inflammasome markers in myocardial tissues of each group (scale bar, 100 $\mu$m). (C) The AOD values of inflammasome markers obtained by immunohistochemical staining. (D) Expression of pyroptotic proteins and HO-1. (E) Quantification of relative mRNA levels of key pyroptotic markers. (F) Semi-quantification of relative expression levels of pyroptotic proteins and HO-1. (G) Protein expression of nuclear NRF2 was assessed by western blotting. (H) Semi-quantification of relative expression levels of NRF2 obtained by western blotting. $^{**}$P<0.01, $^{***}$P<0.001 and $^{****}$P<0.0001 vs. sham group; $^{\#\#\#\#}$P<0.0001 vs. I/R group.. AOD, average optical density; HO-1, heme oxygenase-1; ASC, apoptosis-associated speck-like protein; NLRP3, nucleotide-binding oligomerization domain-like receptor family pyrin domain-containing 3; GSDMD, gasdermin D; Pue, puerarin; I/R, ischemia/reperfusion.

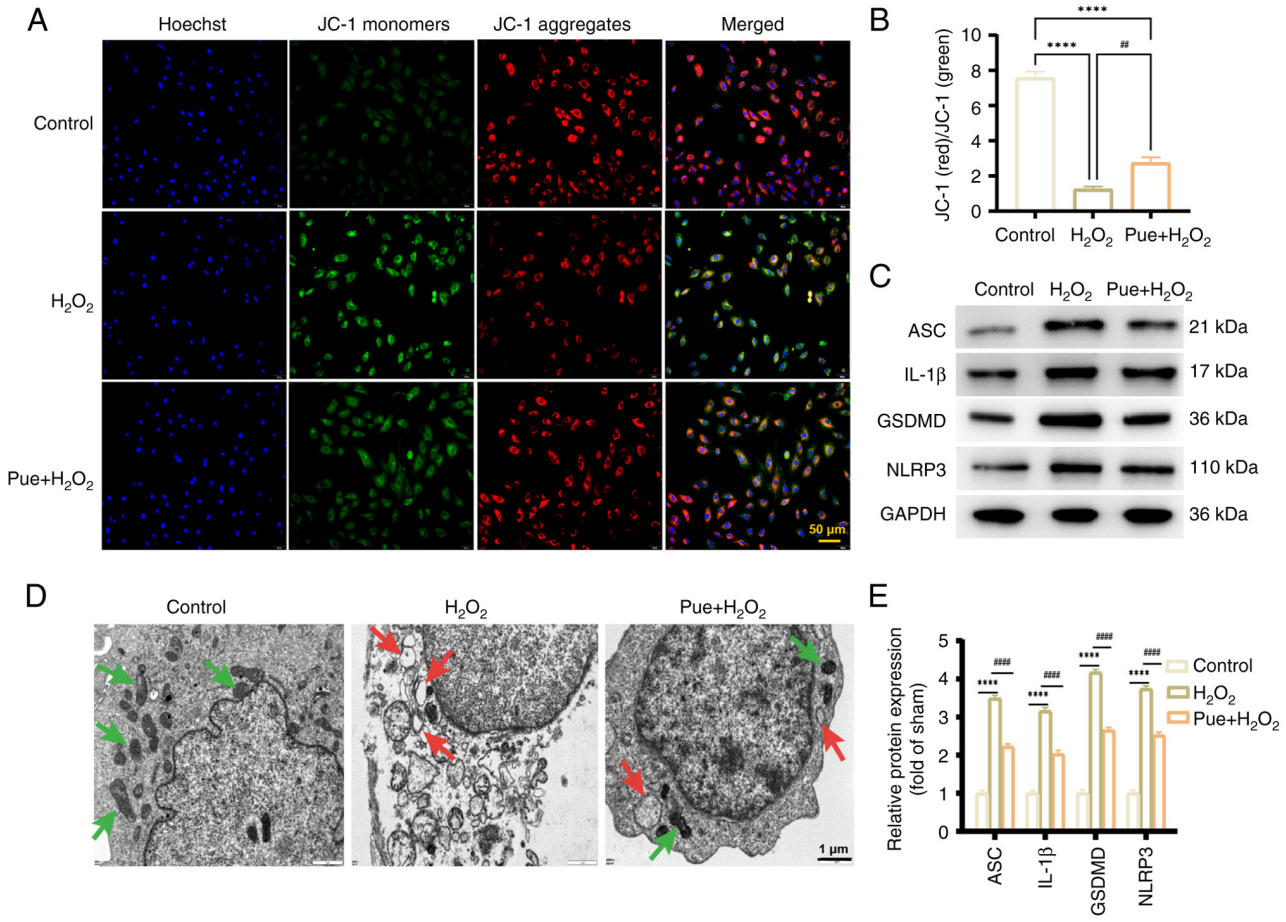


Figure 3. Pue inhibits pyroptosis in cardiomyocytes. (A) JC-1 was used to detect the mitochondrial membrane potential of cardiomyocytes (scale bar, 100 $\mu$m). (B) Quantitative analysis of the ratio of red to green fluorescence. (C) Western blot analysis showed the expression levels of key proteins involved in pyroptosis in cardiomyocytes. (D) Representative morphology of mitochondria obtained by transmission electron microscopy (scale bar, 1 $\mu$m). The green arrow showed normal mitochondria, while the red arrow indicated organelle vacuolation. (E) Semi-quantification of the relative expression levels of key pyroptotic proteins in cardiomyocytes from western blotting results. $^{****}$P<0.0001 vs. control group; $^{\#\#}$P<0.01 and $^{\#\#\#\#}$P<0.0001 vs. $H_2O_2$ group. Pue, puerarin; ASC, apoptosis-associated speck-like protein; GSDMD, gasdermin D; NLRP3, nucleotide-binding oligomerization domain-like receptor family pyrin domain-containing 3.

(Fig. S1C). The morphology of cardiomyocytes was observed by microscope. The morphology of cells in the control group was normal, while cells shrinkage and the number decreased in the $H_2O_2$ group. By contrast, the number of cells in the Pue + $H_2O_2$ group increased significantly (Fig. S1D).

JC-1 staining was used to assess the mitochondrial membrane potential of rat cardiomyocytes. Red fluorescence indicated a high mitochondrial membrane potential, while green fluorescence represented the low mitochondrial membrane potential of cardiomyocytes. Compared with controls, cells in the $H_2O_2$ group exhibited significantly reduced red fluorescence and increased green fluorescence, suggesting a notable decrease in mitochondrial membrane potential. Pue pretreatment was shown to significantly increase the red/green fluorescence ratio compared with the $H_2O_2$ group (Fig. 3A and B). The ultrastructural changes in cells were observed by TEM. In the control group, the morphology and size of mitochondria were normal and mitochondrial cristae were continuous, complete and clearly visible. By contrast, in the $H_2O_2$ group, mitochondria became swollen, with notable loss of cristae, severe vacuolization and nuclear alterations observed, indicating a tendency towards pyroptosis. However, Pue treatment mitigated mitochondrial swelling, disruption of cristae and membrane rupture while restoring nuclear integrity (Fig. 3D). To determine whether the pyroptosis pathway was activated, the expression of key proteins was detected via western blotting. Compared with the control group, the expression levels of NLRP3, ASC, GSDMD and IL-1β were significantly increased in the $H_2O_2$ group. However, the expression of the aforementioned proteins was shown to decrease after Pue treatment. These results indicated that Pue protected H9C2 cells from pyroptosis (Fig. 3C and E).

*Pue activates the NRF2 pathway to protect cardiomyocytes from pyroptosis*. To clarify the possible mechanism by which Pue inhibited cardiomyocyte pyroptosis, the present study constructed an NRF2 overexpression plasmid and verified its expression after transfection via western blotting. The expression of NRF2 in the overexpression plasmid group was significantly higher compared with that in the control plasmid group, indicating a successful construction of the NRF2 overexpression plasmid (Fig. 4A and B). To observe the regulatory effect of Pue on the NRF2/HO-1 signaling pathway, cardiomyocytes were treated with Pue and reclassified into five groups. Immunofluorescence results showed that NRF2 and HO-1 expression levels decreased significantly in control group cells

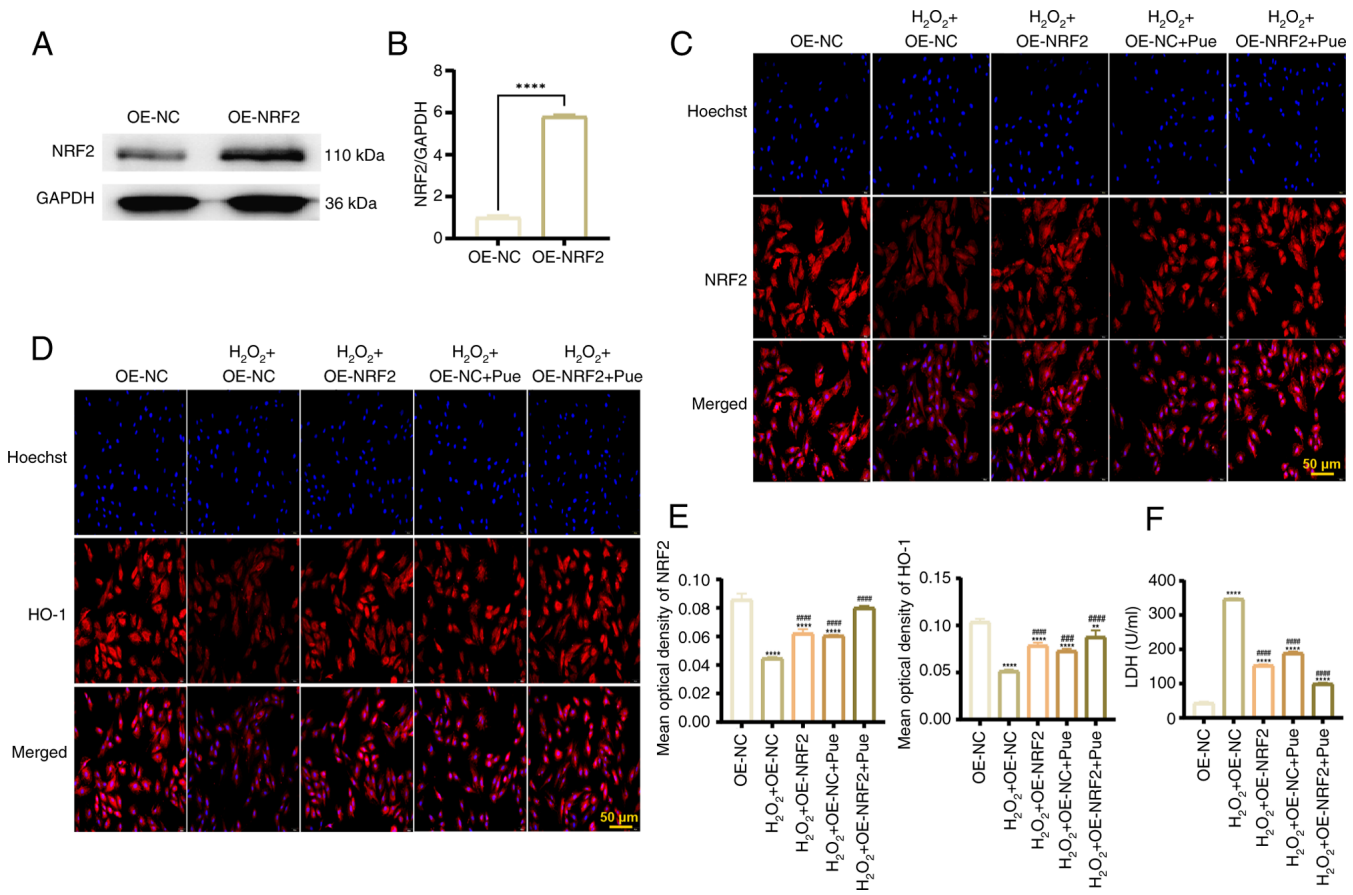


Figure 4. Pue activates the NRF2 pathway to alleviate cardiomyocyte pyroptosis. (A) Western blot assays were used to detect NRF2 expression in cardiomyocytes of the OE-NC group and the OE-NRF2 group (n=3). (B) Semi-quantification of NRF2 protein levels detected in western blotting. (C) Immunofluorescence was used to detect nuclear translocation of NRF2 in each group of cells (n=3). (D) HO-1 expression was detected by immunofluorescence staining in each group of cells (n=3). (E) Quantitative analysis of the fluorescence intensities of NRF2 and HO-1 immunofluorescence staining. (F) Activity of LDH in each group. $^{**}$P<0.01 and $^{****}$P<0.0001 vs. OE-NC group; $^{###}$P<0.001 and $^{####}$P<0.0001 vs. $H_2O_2$ + OE-NC group. OE, overexpression; NC, negative control; NRF2, nuclear factor E2-related factor 2; Pue, puerarin; HO-1, heme oxygenase-1; LDH, lactate dehydrogenase.

after $H_2O_2$ treatment. However, compared with the $H_2O_2$ + OE-NC group, NRF2 was significantly activated in the $H_2O_2$ + OE-NRF2, $H_2O_2$ + OE-NC + Pue and $H_2O_2$ + OE-NRF2 + Pue group. Furthermore, the significantly increased expression of HO-1 in the aforementioned groups suggested that Pue enhanced the nuclear translocation of NRF2 (Fig. 4C-E). During myocardial infarction, the integrity of the cell membrane is damaged, resulting in the release of LDH into the supernatant, which may act as an indirect indication of pyroptosis (19). Based on the results of the LDH release test, the concentration of LDH increased significantly after $H_2O_2$ treatment compared with the OE-NC group. Compared with the $H_2O_2$ + OE-NC group, overexpression of NRF2 or Pue treatment, both individually and in combination, significantly decreased the release of LDH that was influenced by $H_2O_2$ treatment, suggesting that Pue activated NRF2 to exert protective effects on cardiomyocytes (Fig. 4F).

*Pue inhibits $H_2O_2$-induced cardiomyocyte pyroptosis through the NRF2/HO-1 pathway*. To further clarify whether Pue affected pyroptosis via the NRF2/HO-1 pathway, Hoechst 33342/PI staining was used to detect pyroptotic cells. Compared with the OE-NC group, the red fluorescence of cells in the $H_2O_2$ + OE-NC group was significantly enhanced, indicating an increased degree of pyroptosis. However, the red fluorescence of cardiomyocytes significantly decreased after an overexpression of NRF2 or treatment with Pue, suggesting a notable reduction in the proportion of pyroptotic cells following these treatments compared with the $H_2O_2$ + OE-NC group (Fig. 5A and B). Western blot analysis demonstrated that the protein expression of pyroptosis-related proteins NLRP3, ASC, GSDMD, caspase-1 and IL-1β was lower in the $H_2O_2$ + OE-NC + Pue and $H_2O_2$ + OE-NRF2 + Pue groups compared with that in the $H_2O_2$ + OE-NC group. Meanwhile, the protein levels of NRF2 and HO-1 were higher in the aforementioned groups compared with the $H_2O_2$ + OE-NC group (Fig. 5C-F). Under conditions of oxidative stress, Pue appears to have increased NRF2 expression and decreased cardiomyocyte pyroptosis. Thus, Pue was shown to activate the NRF2/HO-1 signaling pathway, thereby inhibiting NLRP3/caspase-1/GSDMD pathway-mediated pyroptosis and protecting cardiomyocytes from injury during MIRI (Fig. 6).

## Discussion

Pue, as the main active component of the traditional Chinese medicine *Pueraria lobata*, has been demonstrated to display multiple protective effects on the cardiovascular system (7).

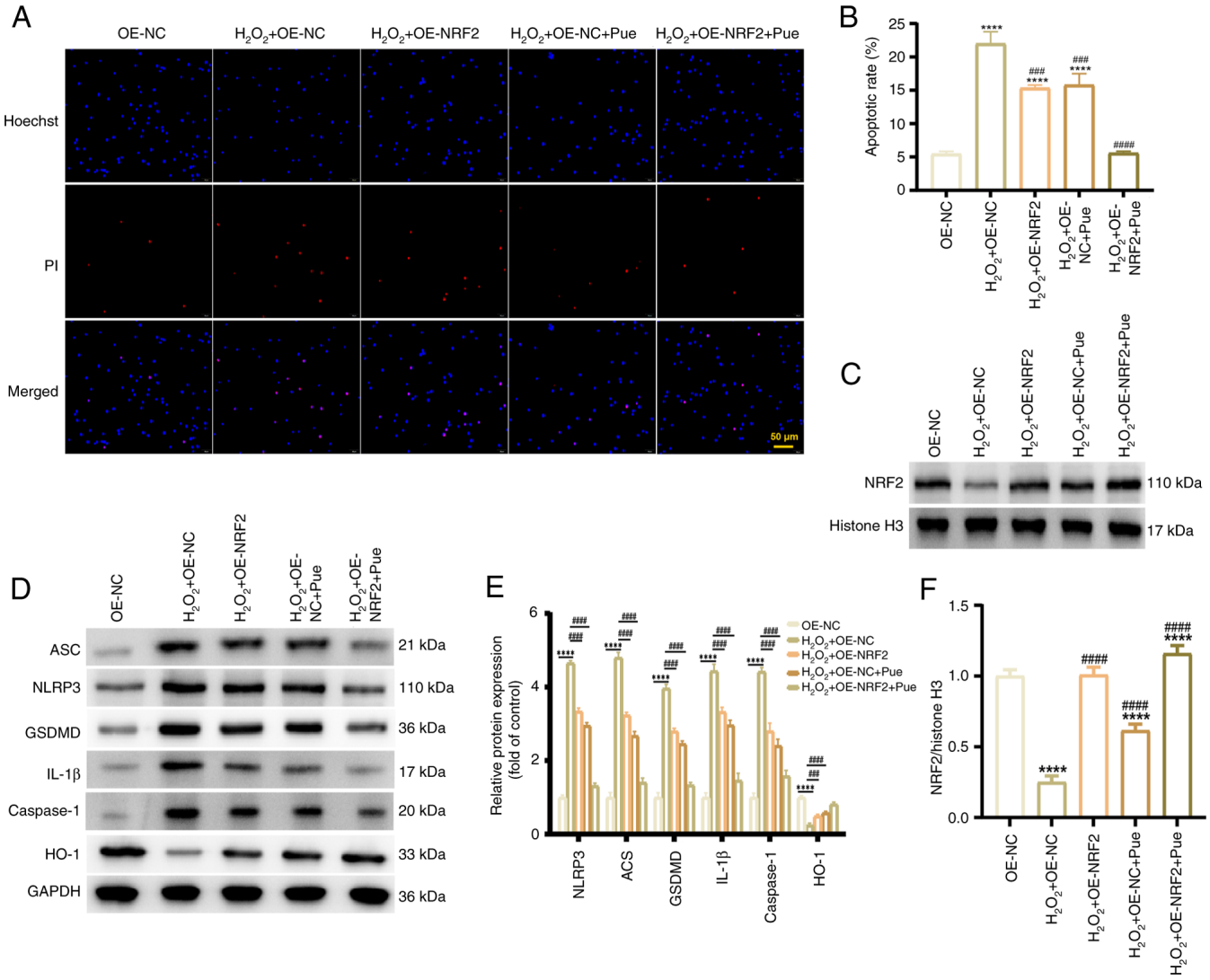


Figure 5. Pue alleviates cardiomyocyte pyroptosis via the NRF2/HO-1 signaling pathway. (A) Hoechst 33342/PI staining detected the apoptotic state of H9C2 cells (magnification, x400) (n=3). (B) Quantitative analysis of PI-positive cells. (C) Western blotting of nuclear NRF2 expression in each group (n=3). (D) Western blotting images of key pyroptotic proteins and HO-1 in each treatment group (n=3). (E) Semi-quantification of the expression of pyroptotic proteins and HO-1 in each group of cells. (F) Semi-quantification of NRF2 protein expression. $^{****}$P<0.0001 vs. OE-NC group; $^{###}$P<0.001 and $^{####}$P<0.0001 vs. $H_2O_2$ + OE-NC group. Pue, puerarin; OE, overexpression; NC, negative control; NRF2, nuclear factor E2-related factor 2; ASC, apoptosis-associated speck-like protein; NLRP3, nucleotide-binding oligomerization domain-like receptor family pyrin domain-containing 3; GSDMD, gasdermin D; HO-1, heme oxygenase-1.

The present study aimed to verify the anti-pyroptotic effect of Pue, exploring its influence on the molecular mechanisms involved in MIRI. Primarily, the present study observed that Pue exhibited a cardioprotective effect on MIRI. Pretreatment with Pue effectively mitigated MIRI-induced myocardial injury, improved cardiac function and partially decreased myocardial fibrosis Additionally, MIRI has been shown to result in elevated oxidative stress and an inflammatory response, accompanied by pyroptosis of cardiomyocytes (20). In the present study, both *in vivo* and *in vitro* experiments demonstrated that Pue reduced the expression of pyroptosis-related proteins and relieved cardiomyocyte pyroptosis, ultimately improving the inflammatory microenvironment. Furthermore, NRF2 activation exhibited cardioprotective effects by regulating HO-1, which is its downstream antioxidant enzyme. The overexpression of NRF2 significantly enhanced the inhibitory effect of Pue on pyroptosis, further validating the importance of this pathway. Therefore, the present study provided a novel theoretical basis for the protective mechanism of Pue during MIRI.

Pyroptosis is a form of programmed cell death that occurs via two pathways: The classical and non-classical pathways. In the classical pyroptotic pathway, NLRP3 serves as a component of the inflammasome, activating caspase-1 via ASC and producing and releasing IL-1β and IL-18. Meanwhile, GSDMD is cleaved into the GSDMD-N terminal domain, which forms a membrane pore that results in cell membrane rupture and pyroptosis (21,22). Inflammasome inhibitors exhibit the potential to reverse the activation of NLRP3 inflammasome-mediated pyroptosis and therefore ameliorate MIRI (23). Inhibition of caspase-1 can reduce myocardial infarct size and cardiac dysfunction caused by MIRI (24). Kawaguchi *et al* (25) also found that in comparison with the control group, ASC- and caspase-1-knockout mice showed

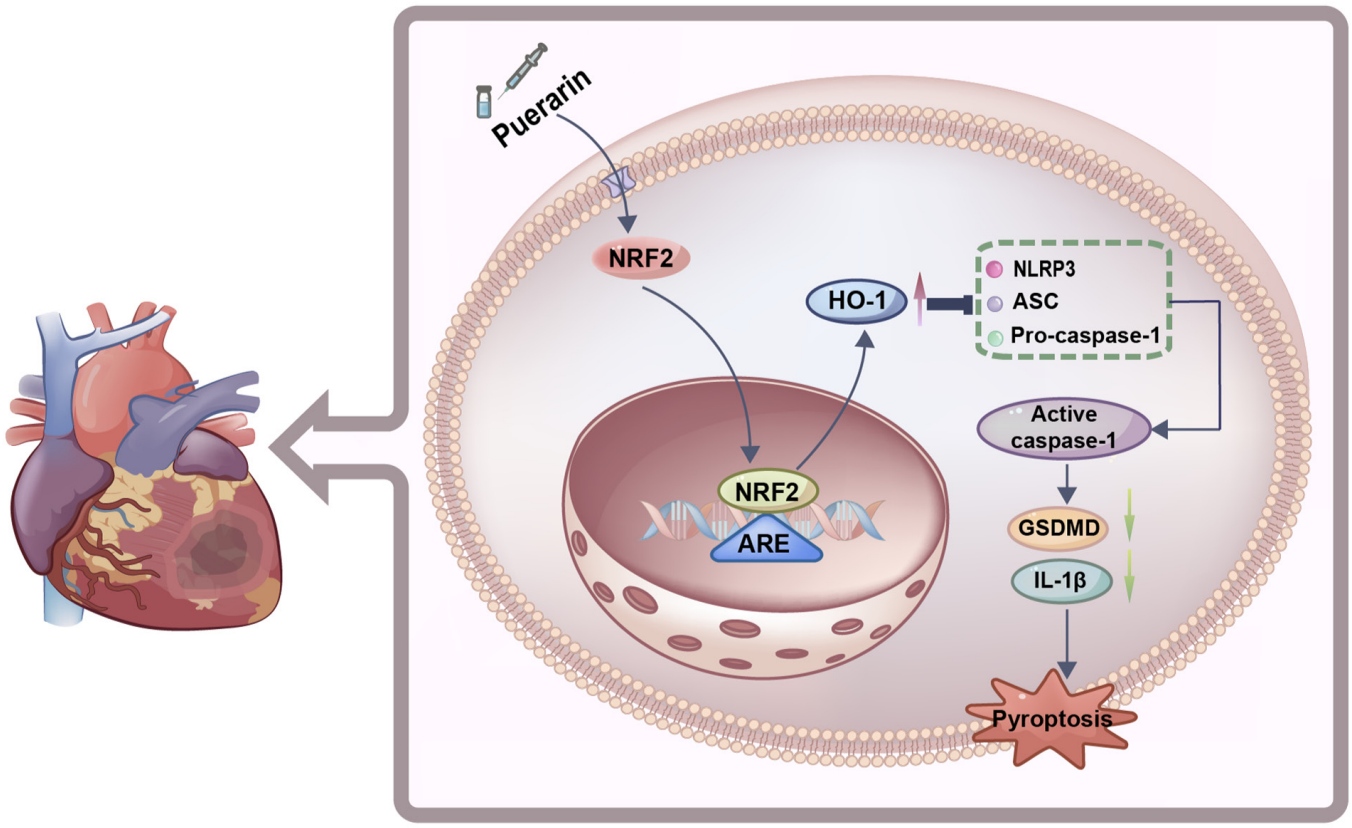


Figure 6. Schematic diagram of the molecular mechanism of Pue-mediated pyroptosis inhibition. NRF2, nuclear factor E2-related factor 2; HO-1, heme oxygenase-1; ARE, antioxidant response element; NLRP3, nucleotide-binding oligomerization domain-like receptor family pyrin domain-containing 3; ASC, apoptosis-associated speck-like protein; GSDMD, gasdermin D.

marked improvements in infarct area formation, myocardial fibrosis and the development of cardiac dysfunction in the setting of MIRI. Consequently, inhibition of pyroptosis has been shown to alleviate myocardial injury caused by I/R.

Pue is a natural flavonoid that exhibits a variety of biological and pharmacological properties (7). In a rat model of sepsis-associated encephalopathy, Pue can inhibit the classical pathway of pyroptosis mediated by NLRP3/caspase-1/GSDMD and alleviate damage to the blood-brain barrier (26). Furthermore, Pue inhibits inflammatory responses and pyroptosis, reduces serum levels of inflammatory cytokines, enhances the antioxidant capacity of the kidneys and improves renal function (27). These protective effects of Pue are associated with the suppression of pyroptosis, mediated through the activation of the AMPK/NAD-dependent protein deacetylase sirtuin-1 (SIRT1) and SIRT1/NLRP3/caspase-1 pathways (28,29). Both the animal and cell models of MIRI displayed increased levels of pyroptotic proteins. In the rat model of myocardial infarction, RT-qPCR showed that the expression levels of the pyroptosis-related proteins ASC, Il-1β, NLRP3 and GSDMD significantly decreased after Pue intervention. Furthermore, western blot analysis also provided evidence that the protein expression levels of NLRP3, ASC, GSDMD, IL-1β and caspase-1 decreased in the Pue group. These results suggested that Pue inhibited cardiomyocyte pyroptosis during MIRI.

In MIRI, mitochondrial dysfunction can result in oxidative stress, apoptosis and pyroptosis (30,31). The relevant literature has reported that Pue recovers impaired mitochondrial membrane potential and ROS levels, thus protecting mitochondrial function (32,33). In the present study, *in vitro* experiments were conducted to establish an oxidative stress model. Here, JC-1 staining showed a significant increase of mitochondrial membrane potential following Pue intervention. Additionally, TEM revealed that Pue could alleviate mitochondrial swelling and the disintegration of inner cristae compared with the $H_2O_2$ control group. This supported the protective effect of Pue on mitochondria. Therefore, the regulatory effect of Pue on mitochondrial function may have also been an important mechanism of pyroptotic inhibition. The increase in HO-1 and NRF2 expression observed in MIRI rats after Pue administration suggested a possible link between Pue, pyroptosis and NRF2 activity, although the underlying mechanism for this requires further exploration.

A large amount of oxygen free radicals, such as superoxide anions and hydroxyl radicals, are produced during MIRI, leading to oxidative stress injury (34,35). The NRF2/HO-1 signaling pathway is an important intracellular antioxidant stress signaling pathway. It is predominantly composed of NRF2 and its target genes, playing a key role in maintaining redox balance within cells and protecting cells from oxidative damage (36,37). In the nucleus, NRF2 binds to the ARE and initiates the transcriptional expression of a series of downstream antioxidant genes. Amongst these, HO-1 is one of the important target genes of NRF2 (38). HO-1 is an inducible enzyme with multiple biological functions. Notably,

HO-1 is capable of catalyzing the decomposition of heme into biliverdin, carbon monoxide and free iron. These metabolites have strong antioxidant effects (39,40). Furthermore, research has found that the expression of the inflammatory factors TNF-α, IL-1 and IL-6 significantly decrease in myocardial tissues after activation of the NRF2/HO-1 signaling pathway, and the infiltration of inflammatory cells is similarly reduced. This shows that the NRF2/HO-1 signaling pathway is capable of inhibiting the inflammatory response in MIRI (41).

LDH is released from cells following pyroptosis due to perforation of the membrane when pyroptosis occurs. Therefore, LDH concentration can be used as an indicator to assess the occurrence of cell membrane damage due to pyroptosis (42). The results of the present study showed that the LDH concentration in the $H_2O_2$ + OE-NRF2 cell group was lower than in the $H_2O_2$ + OE-NC treatment group. Additionally, Hoechst 33342/PI staining showed that the proportion of pyroptotic cells was significantly lower in the $H_2O_2$ + OE-NRF2 than in the $H_2O_2$ + OE-NC group, indicating that NRF2 activation inhibited pyroptosis. Oxidative stress, inflammatory response and pyroptosis appear to exhibit complex interactions. Notably the accumulation of ROS can activate the NLRP3 inflammasome to promote the occurrence of pyroptosis, while the inflammatory factors released during pyroptosis, such as IL-1β, are capable of further exacerbating oxidative stress and the inflammatory response, resulting in the formation of a cycle. Therefore, the NRF2/HO-1 signaling pathway was not only responsible for alleviating oxidative stress injury and inflammation in cardiomyocytes, but was also responsible for inhibiting cardiomyocyte pyroptosis. These results suggested that regulation of the NRF2/HO-1 pathway may become a suitable strategy for preventing pyroptosis.

It has previously been shown that Pue is capable of enhancing the activity of antioxidant enzymes, such as superoxide dismutase and glutathione peroxidase, as well as inhibiting the generation of lipid peroxidation products, eliminating oxygen free radicals and alleviating damage to cardiac muscle cells caused by oxidative stress (43,44). Pue has been shown to regulate the NRF2 pathway and antioxidant enzyme expression in a mouse model of colitis, as well as exert antioxidant properties (45). Pue can also induce the expression of SIRT1, increase the expression of NRF2 and promote the translocation of NRF2 into the nucleus, displaying potential in treating metabolic dysfunction-related fatty liver diseases (46). In a renal I/R model, the expression of NRF2 and HO-1 proteins are increased following injection of Pue, revealing that Pue may mediate its renal protective effects through the NRF2/HO-1 signaling pathway (47). In the present study, NRF2 demonstrated a significant increase in activation and nuclear translocation in the $H_2O_2$ + OE-NC + Pue group compared with the $H_2O_2$ + OE-NC group, suggesting that administration of Pue enhanced NRF2 nuclear translocation. Furthermore, HO-1 expression also increased, indicating that Pue activated the NRF2/HO-1 signaling pathway and enhanced the antioxidant capacity of cardiomyocytes. The expression of pyroptosis-associated proteins was significantly reduced in the Pue-treated groups ($H_2O_2$ + OE-NC + Pue and $H_2O_2$ + OE-NRF2 + Pue) compared with the $H_2O_2$ + OE-NC, suggesting an anti-pyroptotic effect of Pue. This also provides evidence that Pue exerts its anti-pyroptotic effects via the NRF2/HO-1 signaling.

Summarily, the present study, to the best of our knowledge, revealed for the first time the molecular mechanism by which Pue inhibited cardiomyocyte pyroptosis and alleviated MIRI via NRF2/HO-1 pathway regulation. These results not only enrich theories concerning the cardioprotective effect of Pue but also provide a new potential strategy for clinical treatment of MIRI. As a natural drug, Pue has the advantages of low toxicity and wide availability compared with synthetic drugs, such as MCC950. As Pue also interacts with other signaling pathways, such as the PI3K/AKT and MAPK pathways (48,49). Hence, it is necessary to explore the effects produced by these interactions on MIRI. Although the present study did not directly detect cell death pathways, such as apoptosis or necroptosis, Pue has been shown to improve mitochondrial swelling and activate the NRF2/HO-1 pathway. Thus, it was speculated that Pue may indirectly regulate apoptosis by preserving mitochondrial function. Furthermore, understanding the effects of Pue and other therapeutic approaches on different modes of cell death may help to optimize treatment strategies. In the future, Pue can be combined with other existing reperfusion therapies to evaluate drug interactions and ensure the safety of clinical medication.

In conclusion, the present study revealed that Pue inhibited NLRP3/caspase-1/GSDMD-mediated pyroptosis by regulating the NRF2/HO-1 signaling pathway, thereby alleviating myocardial injury during MIRI. *In vivo* and *in vitro* experiments demonstrated that Pue exerted protective effects on cardiac function during MIRI and inhibited pyroptosis of cardiomyocytes, providing evidence for the anti-pyroptotic function of Pue exerted through the NRF2/HO-1 pathway. The findings of the present study provided a promising approach for the treatment of MIRI and offered new insights into the interaction between oxidative stress and pyroptosis.

**Acknowledgements**

Not applicable.

**Funding**

The present work was supported by Youth project of science and technology research program of Chongqing Education Commission of China (grant no. KJQN202302833),the Yunnan Fundamental Research Kunming Medical University Projects (grant no. 202501AY070001-136) and the Natural Science Research Projects of Chongqing Medical and Pharmaceutical College (grant no. YGZZK2025104).

**Availability of data and materials**

The data generated in the present study may be requested from the corresponding author.

**Authors' contributions**

XZ and YD designed the study. XZ performed the main experiments. JL, TH, LT and DL were responsible for data

analysis. XZ and YD confirm the authenticity of all the raw data. All authors read and approved the final version of the manuscript.

## Ethics approval and consent to participate

All protocols in the present study strictly complied with the ethical guidelines for animal research, and the animal experiment procedures were reviewed and approved by the Ethics Committee of Chongqing Medical University (Chongqing, China; approval no. IACUC-CQMU-2024-0618).

## Patient consent for publication

Not applicable.

## Competing interests

The authors declare that they have no competing interests.

## References


1. Heusch G: Myocardial ischemia/reperfusion: Translational pathophysiology of ischemic heart disease. Med 5: 10-31, 2024.
2. Sánchez-Hernández CD, Torres-Alarcón LA, González-Cortés A and Peón AN: Ischemia/reperfusion injury: Pathophysiology, current clinical management, and potential preventive approaches. Med Inflamm 2020: 8405370, 2020.
3. Zhang S, Yan F, Luan F, Chai Y, Li N, Wang YW, Chen ZL, Xu DQ and Tang YP: The pathological mechanisms and potential therapeutic drugs for myocardial ischemia reperfusion injury. Phytomedicine 129: 155649, 2024.
4. Toldo S and Abbate A: The role of the NLRP3 inflammasome and pyroptosis in cardiovascular diseases. Nat Rev Cardiol 21: 219-237, 2024.
5. Vasudevan SO, Behl B and Rathinam VA: Pyroptosis-induced inflammation and tissue damage. Semin Immunol 69: 101781, 2023.
6. He J, Liu D, Zhao L, Zhou D, Rong J, Zhang L and Xia Z: Myocardial ischemia/reperfusion injury: Mechanisms of injury and implications for management (review). Exp Ther Med 23: 430, 2022.
7. Jiang Z, Cui X, Qu P, Shang C, Xiang M and Wang J: Roles and mechanisms of puerarin on cardiovascular disease: A review. Biomed Pharmacother 147: 112655, 2022.
8. Gao M, Zhang Z, Lai K, Deng Y, Zhao C, Lu Z and Geng Q: Puerarin: A protective drug against ischemia-reperfusion injury. Front Pharmacol 13: 927611, 2022.
9. Lyu Q, Xue W, Liu R, Ma Q, Kasaragod VB, Sun S, Li Q, Chen Y, Yuan M, Yang Y, *et al*: A brain-to-gut signal controls intestinal fat absorption. Nature 634: 936-943, 2024.
10. Wang K, Sun Y, Zhu K, Liu Y, Zheng X, Yang Z, Man F, Huang L, Zhu Z, Huang Q, *et al*: Anti-pyroptosis biomimetic nanoplatform loading puerarin for myocardial infarction repair: From drug discovery to drug delivery. Biomaterials 314: 122890, 2025.
11. Sun S, Gong D, Liu R, Wang R, Chen D, Yuan T, Wang S, Xing C, Lv Y, Du G and Fang L: Puerarin Inhibits NLRP3-Caspase-1-GSDMD-Mediated Pyroptosis via P2X7 receptor in cardiomyocytes and macrophages. Int J Mol Sci 24: 13169, 2023.
12. Zhang Q, Liu J, Duan H, Li R, Peng W and Wu C: Activation of Nrf2/HO-1 signaling: An important molecular mechanism of herbal medicine in the treatment of atherosclerosis via the protection of vascular endothelial cells from oxidative stress. J Adv Res 34: 43-63, 2021.
13. Qiu Z, He Y, Ming H, Lei S, Leng Y and Xia ZY: Lipopolysaccharide (LPS) aggravates high Glucose- and Hypoxia/reoxygenation-induced injury through activating ROS-Dependent NLRP3 Inflammasome-mediated pyroptosis in H9C2 cardiomyocytes. J Diabetes Res 2019: 8151836, 2019.
14. Zhang J, Pan W, Zhang Y, Tan M, Yin Y, Li Y, Zhang L, Han L, Bai J, Jiang T and Li H: Comprehensive overview of Nrf2-related epigenetic regulations involved in ischemia-reperfusion injury. Theranostics 12: 6626-6645, 2022.
15. Jiang S, Qiu S, Mu Y, Liu C, Han Y, Jiang J and Wang Y: Puerarin reduces susceptibility to ventricular arrhythmias and inhibits ferroptosis via Sirt1/Nrf2 signaling in high-fat-diet rats. Free Radic Biol Med 227: 472-484, 2025.
16. MacArthur Clark JA and Sun D: Guidelines for the ethical review of laboratory animal welfare People's Republic of China National Standard GB/T 35892-2018 [Issued 6 February 2018 Effective from 1 September 2018]. Animal Model Exp Med 3: 103-113, 2020.
17. Chen L, Mao LS, Xue JY, Jian YH, Deng ZW, Mazhar M, Zou Y, Liu P, Chen MT, Luo G and Liu MN: Myocardial ischemia-reperfusion injury: The balance mechanism between mitophagy and NLRP3 inflammasome. Life Sci 355: 122998, 2024.
18. Zhang AY, Su JB, Sun HT, Liu Q, Li R, Zhang Y, Wang Y, Wang MY, Ji LM, Gao SQ, *et al*: Stachyose ameliorates myocardial ischemia-reperfusion injury by inhibiting cardiomyocyte ferroptosis and macrophage pyroptosis. Int Immunopharmacol 143: 113334, 2024.
19. Luo T, Jia X, Feng WD, Wang JY, Xie F, Kong LD, Wang XJ, Lian R, Liu X, Chu YJ, *et al*: Bergapten inhibits NLRP3 inflammasome activation and pyroptosis via promoting mitophagy. Acta Pharmacol Sin 44: 1867-1878, 2023.
20. Pagliaro P and Penna C: Inhibitors of NLRP3 inflammasome in ischemic heart disease: Focus on functional and redox aspects. Antioxidants (Basel) 12: 1396, 2023.
21. Coll RC, Schroder K and Pelegrín P: NLRP3 and pyroptosis blockers for treating inflammatory diseases. Trends Pharmacol Sci 43: 653-668, 2022.
22. Broz P and Dixit VM: Inflammasomes: Mechanism of assembly, regulation and signalling. Nat Rev Immunol 16: 407-420, 2016.
23. Zhang L, Jiang YH, Fan C, Zhang Q, Jiang YH, Li Y and Xue YT: MCC950 attenuates doxorubicin-induced myocardial injury in vivo and in vitro by inhibiting NLRP3-mediated pyroptosis. Biomed Pharmacother 143: 112133, 2021.
24. Liao Y, Liu K and Zhu L: Emerging roles of inflammasomes in cardiovascular diseases. Front Immunol 13: 834289, 2022.
25. Kawaguchi M, Takahashi M, Hata T, Kashima Y, Usui F, Morimoto H, Izawa A, Takahashi Y, Masumoto J, Koyama J, *et al*: Inflammasome activation of cardiac fibroblasts is essential for myocardial ischemia/reperfusion injury. Circulation 123: 594-604, 2011.
26. Zhou S, Li Y, Hong Y, Zhong Z and Zhao M: Puerarin protects against sepsis-associated encephalopathy by inhibiting NLRP3/caspase-1/GSDMD pyroptosis pathway and reducing blood-brain barrier damage. Eur J Pharmacol 945: 175616, 2023.
27. Wang K, Tang Z, Liu S, Liu Y, Zhang H and Zhan H: Puerarin protects renal ischemia-reperfusion injury in rats through NLRP3/Caspase-1/GSDMD pathway. Acta Cir Bras 38: e387323, 2023.
28. Wang L, Xie X, Chen Q, Chen Y, Xu X and Liang T: Puerarin reduces diabetic nephropathy-induced podocyte pyroptosis by modulating the SIRT1/NLRP3/caspase-1 pathway. Mol Cell Endocrinol 595: 112409, 2025.
29. Peng ZT and Liu H: Puerarin attenuates LPS-induced inflammatory injury in gastric epithelial cells by repressing NLRP3 inflammasome-mediated apoptosis. Toxicol In Vitro 81: 105350, 2022.
30. Chang X, Liu J, Wang Y, Guan X and Liu R: Mitochondrial disorder and treatment of ischemic cardiomyopathy: Potential and advantages of Chinese herbal medicine. Biomed Pharmacother 159: 114171, 2023.
31. Peng JF, Salami OM, Lei C, Ni D, Habimana O and Yi GH: Targeted mitochondrial drugs for treatment of myocardial ischaemia-reperfusion injury. J Drug Target 30: 833-844, 2022.
32. Niu P, Sun Y, Wang S, Li G, Tang X, Sun J, Pan C and Sun J: Puerarin alleviates the ototoxicity of gentamicin by inhibiting the mitochondria-dependent apoptosis pathway. Mol Med Rep 24: 851, 2021.
33. Sheng G, Wu Y, Yao L, Liu H, Zhang P, Song C, Wu G and Zhu H: Puerarin improves the comorbidity of chronic pain and depression by binding with Bax and reducing mitochondrial dysfunction. Mol Pain 21: 17448069251335230, 2025.
34. Dhalla NS, Shah AK, Adameova A and Bartekova M: Role of oxidative stress in cardiac dysfunction and subcellular defects due to ischemia-reperfusion injury. Biomedicines 10: 1473, 2022.
35. Xiang M, Lu Y, Xin L, Gao J, Shang C, Jiang Z, Lin H, Fang X, Qu Y and Wang Y: Role of oxidative stress in reperfusion following myocardial ischemia and its treatments. Oxid Med Cell Longev 2021: 6614009, 2021.

36. Geng J and Zhang C: Liensinine attenuates inflammatory response and oxidative stress by activation of Nrf2/HO-1 signaling in L-NAME-induced gestational hypertension. Naunyn Schmiedebergs Arch Pharmacol 398: 14089-14098, 2025.
37. El-Emam SZ, Soubh AA, Al-Mokaddem AK and Abo El-Ella DM: Geraniol activates Nrf-2/HO-1 signaling pathway mediating protection against oxidative stress-induced apoptosis in hepatic ischemia-reperfusion injury. Naunyn Schmiedebergs Arch Pharmacol 393: 1849-1858, 2020.
38. Yang X, Liu Y, Cao J, Wu C, Tang L, Bian W, Chen Y, Yu L, Wu Y, Li S, *et al*: Targeting epigenetic and post-translational modifications of NRF2: Key regulatory factors in disease treatment. Cell Death Discov 11: 189, 2025.
39. Kuo PC, Weng WT, Scofield BA, Paraiso HC, Yu II and Yen JJ: Ischemia-induced endogenous Nrf2/HO-1 axis activation modulates microglial polarization and restrains ischemic brain injury. Front Immunol 15: 1440592, 2024.
40. Manavi MA, Mohammad Jafari R, Shafaroodi H and Dehpour AR: The Keap1/Nrf2/ARE/HO-1 axis in epilepsy: Crosstalk between oxidative stress and neuroinflammation. Int Immunopharmacol 153: 114304, 2025.
41. Sun YY, Zhu HJ, Zhao RY, Zhou SY, Wang MQ, Yang Y and Guo ZN: Remote ischemic conditioning attenuates oxidative stress and inflammation via the Nrf2/HO-1 pathway in MCAO mice. Redox Biol 66: 102852, 2023.
42. Shi Y, Yang Y, Xu W, Shi D, Xu W, Fu X, Lv Q, Xia J and Shi F: E3 ubiquitin ligase SYVN1 is a key positive regulator for GSDMD-mediated pyroptosis. Cell Death Dis 13: 106, 2022.
43. Huang Y, Wu H, Hu Y, Zhou C, Wu J, Wu Y, Wang H, Lenahan C, Huang L, Nie S, *et al*: Puerarin attenuates oxidative stress and ferroptosis via AMPK/PGC1α/Nrf2 pathway after subarachnoid hemorrhage in rats. Antioxidants (Basel) 11: 1259, 2022.
44. Hou BY, Zhao YR, Ma P, Xu CY, He P, Yang XY, Zhang L, Qiang GF and DU GH: Hypoglycemic activity of puerarin through modulation of oxidative stress and mitochondrial function via AMPK. Chin J Nat Med 18: 818-826, 2020.
45. Jeon YD, Lee JH, Lee YM and Kim DK: Puerarin inhibits inflammation and oxidative stress in dextran sulfate sodium-induced colitis mice model. Biomed Pharmacother 124: 109847, 2020.
46. Yang M, Xia L, Song J, Hu H, Zang N, Yang J, Zou Y, Wang L, Zheng X, He Q, *et al*: Puerarin ameliorates metabolic dysfunction-associated fatty liver disease by inhibiting ferroptosis and inflammation. Lipids Health Dis 22: 202, 2023.
47. Wang J, Zheng Q, Chen Z, Liu X, Wan S and Wang L: Puerarin alleviates renal ischemia/reperfusion injury by inhibiting apoptosis and endoplasmic reticulum stress via Nrf2/HO-1 pathway. Iran J Basic Med Sci 28: 187-193, 2025.
48. Chen ZQ, Zhou Y, Huang JW, Chen F, Zheng J, Li HL, Li T and Li L: Puerarin pretreatment attenuates cardiomyocyte apoptosis induced by coronary microembolization in rats by activating the PI3K/Akt/GSK-3β signaling pathway. Korean J Physiol Pharmacol 25: 147-157, 2021.
49. Wang Z, Yu Y, Shao W, Zhao Y, Li Z, Han J, Wen J, Meng Y, Lin Y and Wang S: Puerarin ameliorates alcoholic liver disease by regulating intestinal flora and MAPK/Nrf2 signalling pathways. Ecotoxicol Environ Saf 309: 119699, 2026.